

Distributed Sensor Networks for Detection of Mobile Radioactive Sources

Robert J. Nemzek, Jared S. Dreicer, David C. Torney

Abstract--The ability to track illicit radioactive transport through an urban environment has obvious national security applications. This goal may be achieved by means of individual portal monitors, or by a network of distributed sensors. We have examined the distributed sensing problem by modeling a network of scintillation detectors measuring a Cesium-137 source. We examine signal-to-noise behaviors that arise in the simple combination of data from networked radiation sensors. We find that, in the ideal case, large increases in signal-to-noise compared to an individual detector can be achieved, even for a moving source. We also discuss statistical techniques for localizing and tracking single and multiple radioactive sources.

I. INTRODUCTION

THE distributed sensor network project at Los Alamos National Laboratory is investigating the use of networked detection for various applications, including tracking of radioactive materials. Currently proposed solutions to the detection of radioactive materials in an urban setting typically involve the use of individual, large, portal-monitor-style detectors positioned at choke points. This may not ultimately be acceptable in an urban environment, given the large number of transport avenues to be covered and the potential objections to large detection packages; a more discreet solution may be required. We therefore are investigating the use of large numbers of small detectors. We are not attempting here to answer the question of whether detection limits, for example, are better or worse in such a situation, compared to a portal monitor scenario. We are only examining the characteristics, specifically signal-to-noise (SNR), to be expected in a distributed network. We assume that the detectors in our system are stand-alone and wirelessly networked to allow immediate data sharing with freedom from the need for an infrastructure (external power, cables, internet connections, etc.). We furthermore assume that such a sensor network would be devised as an independent and fully distributed entity, not requiring a centralized processing

station. This is achievable by using a microcontroller built into the individual sensing nodes; or by incorporating dedicated processing nodes into the network, in cases where more processing power is required than can be conveniently fitted into the sensors themselves. The Distributed Sensor Network, or DSN, then, consists of a large number of small, simple detector/processor nodes with the capability of sharing either raw or partially-processed data. The data are autonomously analyzed by the network. This is done either by individual nodes collecting data (through some combination of automatic publishing and requesting), or through the use of a software agent traveling through the network, collecting relevant data and calculating partial results as it goes.

In addition to the radiation detectors themselves, the sensor nodes on the network would probably be equipped with GPS receivers for time synchronization and position information. A complete detection package could be built with low enough power requirements to allow long-term operation on battery power. The addition of a solar recharge system would permit a system capable of long-term autonomous monitoring to be fielded on short notice, for example at special events or in response to particular threats. Such a system would require ad-hoc networking capabilities, as are being researched at a number of institutions. Finally, any deployed system would need mechanisms for tagging suspect vehicles (e.g., a triggered video system), and alerting authorities to a potential threat.

II. SIGNAL-TO-NOISE FOR A SINGLE DETECTOR

Our chosen scenario: a radioactive source is traveling at constant speed parallel to a line of evenly-spaced identical detectors. This is a simple geometry, but does represent an urban or roadside situation. We take the source to be a small quantity of Cesium-137; this isotope was chosen because its availability in industrial sources and typical powdered form (as CsCl) make it a potential element of a radiological dispersal device ("dirty bomb"). The source is described by its speed, distance of closest approach to any particular detector, and activity. Any actual device being transported would have both intentional and intrinsic shielding; for convenience, we define the activity of the source to be its equivalent (in terms of number of gammas/s escaping the vehicle) in an unshielded condition. We choose as our detectors the ubiquitous 75mm NaI scintillator. The source-to-detector response function in the model includes the inverse square fall-off, atmospheric attenuation, and factors for the capture and conversion in the NaI of gammas into pulses within the Cs-137 photopeak (662 keV). Edge effects, angular response, and any sources of electronic noise are ignored, as we are most concerned with

Manuscript received October 21, 2003. This work was supported by the U.S. Department of Energy/NNSA and Los Alamos National Laboratory Laboratory Directed Research and Development funds under University of California Contract W-7405-ENG-36.

R. J. Nemzek is with the Los Alamos National Laboratory, ISR-4, MS-D448, Los Alamos, NM 87545 USA (telephone: 505-667-0822, e-mail: Nemzek@lanl.gov).

J. S. Dreicer is with the Los Alamos National Laboratory, DIR, MS-D440, Los Alamos, NM 87545 USA. (telephone: 505-667-0005, e-mail: jdreicer@lanl.gov).

D. C. Torney is with the Los Alamos National Laboratory, T-10, MS-K710, Los Alamos, NM 87545 USA, (telephone: 505-667-9452, e-mail: dct@lanl.gov).

discovering the overall features of the SNR, rather than with calculating the exact SNR for a specific sensor. We assume an array of 25 detectors in a straight, level line, with constant 10m separation between individual detectors.

To calculate the SNR for a single detector, we start by calculating an “interaction length,” the product of the source speed and the detector’s integration time. We consider this interaction length to be centered on the middle detector in the array. The source is then propagated from one end of the interaction length to the other at the chosen speed, and count rates are calculated and integrated in 10ms bins for the duration of the integration time, at which time the source has reached the far end of the interaction length. We also include a constant background level of 7 counts/s under the photopeak, derived from published natural background spectra [1]. SNR is then calculated as $(S / \sqrt{S + B})$, where S represents the integrated count rate from the source, and B the integrated counts due to background. If background levels are changing in a non-statistical fashion, it may be appropriate to calculate SNR as simply $(S / (\sqrt{S} + B))$ [2,3]. We have retained the standard definition; the difference is minor for the situations we are considering.

Ordinarily, SNR would increase with the square root of the detector integration time. But this is not the case when considering a moving source. As the integration time increases, the source spends more and more time increasingly far from the detector, reducing the average count rate; the situation worsens as the speed of the source increases. Fig. 1, the results of one set of our calculations, bears this out. In Fig. 1, shading indicates calculated SNR: white represents high SNR. As the speed of the source (horizontal axis) increases, the SNR always drops. As the integration time is increased (vertical axis), the SNR increases at first, then drops. This effect is most easily seen at moderately high source speeds. The net effect is that, for any given source speed, there is an integration time that maximizes the SNR. This is clearly seen by examining the solid contour lines; the peak SNR for a given speed is at the “nose” of a contour. This result can also be derived by means of an analytical approximation; [4] used the expression $T = 2.8L/V$ (T =integration time, L =distance of closest approach, V =source speed). Likewise, the locus of points of maximum SNR in Fig. 1, shown by the dotted line, follows an L/V hyperbola, with a coefficient of 12. A change in any of the parameters of our model (closest approach, source activity, detector type, background, gamma energy, and so on) would alter the specifics of the SNR curves from that demonstrated by Fig. 1, but the general behavior (maximum SNR at an integration time given by a hyperbolic curve) would remain the same.

III. SIGNAL-TO-NOISE FOR NETWORKED DETECTORS

Next we examine the increase in SNR made possible by adding together detector outputs. We make the assumption that all 25 detectors in the network are operating identically, with synchronized integration times, and with identical background levels. One detector (the 13th or central unit) is treated as in the previous section, i.e., it is the detector on which the

interaction length happens to be centered. The calculation of SNR for the surrounding detectors is performed as before, with the exception that the center of the interaction length is displaced some distance to one side or the other. We assume that the integrated counts from each detector are all made available at some point in the network. We then add the SNR values in quadrature for varying numbers of detectors: 1 (central detector), 3 (center plus one on each side), 5 (center plus two on each side), and so on, to a total of 25 detectors.

Typical results are shown in Fig. 2, expressed as a ratio of SNR for the combined detectors to SNR for a single detector. The top half of Fig. 2 is for a source speed of 20 m/s, while the bottom half is for a source speed of 10 m/s. Each curve on the plots represents a different integration time. For each integration time, the SNR ratio increases as the number of detectors increases. After some number of detectors is added, however, the SNR ratio curve flattens out. This occurs because the additional detectors are increasingly far from the interaction length of the source, and therefore the integrated background is relatively larger. As the interaction length is increased (compare curves at increasing integration times in either panel, or the same integration time in both panels), the greater the number of detectors that can be added before the roll-off occurs. At the longest interaction lengths shown in Fig. 2 (integration times of 50 s and 100 s), the SNR ratio curve collapses into a straight line (on our log-log plot) for all detector combinations. This line is simply the \sqrt{N} (where N is the number of detectors) increase one would expect from the statistics of adding collocated detectors. The motion of the source combined with the integration time has made the detectors virtually collocated. The curves in Fig. 2 are symmetric with respect to integration time and speed; that is, the SNR ratio curve for a 1-s integration time and a source moving at 10m/s is identical to the curve for a 10-s integration time and a 1 m/s source speed. Only their product, the interaction length, matters. In Fig. 2, the curves for higher speeds are above those for lower speeds, at any given integration time. This does not contradict the results of the previous section that source speed reduces SNR, since Fig. 2 presents a ratio of SNRs. If absolute SNR values were plotted, the SNR for some number of combined detectors and a high speed source would be lower than that for the same number of detectors and a low-speed source. Some situations might have a cross-over where a curve that has leveled off intercepts one that is still increasing.

With a system of networked detectors capable of autonomous storage and trading of data, it is straightforward to do something more complicated than what was described in the previous paragraph: the coherent addition of data. By “coherent addition,” we mean the combination of data values while taking into account the motion of the source: the counts from each detector are added together with increasing time lags, so that (hopefully) the integration window follows the source as it moves from detector to detector. We simulated this in our model by propagating the source past the detector array in a series of contiguous interaction lengths (again, we are assuming that the detectors are integrating in synchronization). We first selected the integration interval that provided the maximum SNR for the central (13th) detector in our array of

25. We then added detectors with zero lags (same situation as Fig. 2), 1 lag (nearest neighbors to the center are combined using the integration time 1 step ahead or behind the center, 2nd nearest neighbors 2 steps ahead or behind, etc.), 2 lags (nearest neighbors 2 steps removed, 2nd nearest neighbors 4 steps removed, etc.), and so on. Detectors are combined in groups totalling 1, 3, 5, ..., 25 as before. Again, the data values were added in quadrature and SNR calculated; the results are presented in Fig. 3. When the interaction length matches the detector spacing and number of lags (Fig. 3, upper panel, 1 lag), the SNR increases along the \sqrt{N} curve without limit. There is no roll-off as the number of detectors is increased, as coherent addition process keeps the source centered on the integration time window of each detector. Under less favorable conditions, (lower panel, 1 lag) the SNR increases with the combination of a few detectors, then rolls off. For very poor matches (lower panel, lags=3,4,5), the SNR for combined detectors is always worse than that of a single detector.

Finally, in Fig. 4, we see the effect of a varying speed on the coherent integration process. We start with a situation in which the lag factor is chosen to produce an exact match with the source speed, giving a linearly increasing SNR ratio on the log-log plot. As a small, constant acceleration is introduced (0.02m/s² and 0.1m/s² are shown), the SNR ratio begins to break away from the \sqrt{N} curve, with the effect increasing as more detectors are combined. In this demonstration, the initial speed of the source was chosen so that the accelerating source was moving at 10 m/s as it passed the 25th detector in the array, after an elapsed time of 100s. The loss in SNR is approximately 50% for 25 detectors and an acceleration of 0.1m/s².

IV. BAYESIAN METHODS FOR RADIOACTIVE-SOURCE LOCALIZATION

The key to Bayesian methods is a formula for the probability of the data- the counts recorded at the sensors, c_s ; $s=1,2,...,S$, given the level of background radiation, b , and the source's parameters: were it stationary, these would be its coordinates, say, (x, y) , and its amplitude (or strength) a . Here we assume that Poisson statistics obtain, and, therefore (from its convolution properties) the desired formula is

$$\Pr(c_1, c_2, \dots, c_s \mid x, y, a, b) = \prod_{s=1}^S \exp\{-\mu_s\} \frac{\mu_s^{c_s}}{c_s!} \quad (1)$$

where

$$\mu_s \stackrel{\text{def}}{=} \frac{a}{r_s^2} + b,$$

with r_s denoting the Euclidean distance between the source and sensor node s ; $s=1,2,...,S$.

Although (1), along with a suitable prior distribution, specifies a posterior distribution of (x, y, a) , given the data, the characterization of this distribution through its moments, for instance $\langle x \rangle$, $\langle y \rangle$ and $\langle a \rangle$, could be salutary. That is, the sensor network could automatically compute these expected

values and, under appropriate circumstances, forward these—to narrow the search for a putative radioactive source. Adaptive Gaussian quadrature may be used to evaluate the respective integrals. Analogous techniques apply to a moving source and to multiple sources. (For which one should invoke “partitions” of the counts into those belonging to each source and accommodate nearly-everywhere vanishing integrands. The Markov chain Monte Carlo (MCMC) method may be used to effect the “importance sampling” of good partitions [5].) At the expense of an increase in the complexity of the probability distributions to be calculated, the Bayesian framework can also be used for source tracking and with spectral data [6,7].

V. CONCLUSION

The signal-to-noise that can be expected from a single detector measuring a moving source is considerably different from what is expected for a stationary source: there is an optimal integration time which is proportional to the ratio of closest-approach-distance to source-speed. When combining readings of a moving source from an array of detectors, we find that SNR increases along a \sqrt{N} curve for small numbers of detectors, but levels off for larger numbers of detectors, with the position of the roll-off depending on the “interaction length,” given by the product of source speed and integration time. This limitation can be overcome by incorporating appropriate time lags into the addition, such that the integration windows used in the addition follows the source as it moves from detector to detector. Sophisticated analyses such as Bayesian tracking and the MCMC method may be employed for source estimation, location, and tracking as well as the separation of multiple sources.

A small detector will always have lower efficiency than a large detector, although in the presence of background the two may be equivalent in detection abilities [3]. For a detector array, the coherent addition process can make up for the low efficiency of small detectors. The difficulty, of course, is that the sensor network must have some knowledge of the traffic speed to determine the appropriate time lag for addition. The sensor network design could easily incorporate an average speed measurement, or even a vehicle-specific speed in areas of low traffic density. Alternatively, if the traffic speed is relatively constant, the sensor network's data fusion algorithm could simply step through different lag values; as Fig. 3 demonstrates, there will be a relatively limited set of reasonable values, and a rapid improvement in SNR at the correct one. In any event, the increasing SNR shown in Fig. 3 would not be sustained indefinitely in a real-world situation.

The coherent addition process is a simple, and well within the processing and data storage capabilities of simple distributed sensor systems. A system incorporating Bayesian or MCMC methods may require the addition of dedicated processing nodes to provide the compute power needed for a timely decision. The results shown here demonstrate that the system design for a radioactivity-detecting DSN will have clear choices for at least two important parameters: the integration time for a single detector and the maximum number of detector outputs that need to be combined at any one location. In an operational system, both of these quantities may have to be

adaptive, as they depend on the speed of the source being detected.

VI. REFERENCES

- [1] R. R. Finck, K. Liden, and R. B. R. Persson, "In situ measurements of environmental gamma-radiation by use of a Ge(Li) spectrometer," *Nuc. Instrum. Meth.*, v. 135, no. 3, pp. 559-567, 1976.
- [2] G. F. Knoll, *Radiation Detection and Measurement*, 3rd ed., New York: John Wiley and Sons, 2000, pp. 785-787.
- [3] K. P. Ziocck and W. H. Goldstein, "The lost source, varying backgrounds and why bigger may not be better," in *Unattended Radiation Sensor Systems for Remote Applications*, J. I. Trombka, Ed., New York: American Institute of Physics, 2002, pp. 60-70.
- [4] G. M. Worth, C. N. Henry, R. D. Hastings, and S. W. France, "A portable gamma-ray detection system for location of radioactive sources," *Los Alamos National Laboratory Report LA-UR-76-1241*, Los Alamos National Laboratory, Los Alamos, NM, 1976.
- [5] E. Knill, A. Schliep, and D. C. Torney, "Interpretation of pooling experiments for screening a clone map," *J. Comp. Biol.*, v. 3, pp. 395-406, 1996.
- [6] C. T. Cunningham, "Detection and tracking of a stochastic target using multiple measurements," Lawrence Livermore National Laboratory Report UCRL-ID-122786, Lawrence Livermore National Laboratory, Livermore, CA, 1995.
- [7] C. T. Cunningham, "Bayesian spectroscopy and target tracking," Lawrence Livermore National Laboratory Report UCRL-143305, Lawrence Livermore National Laboratory, Livermore, CA, 2001.

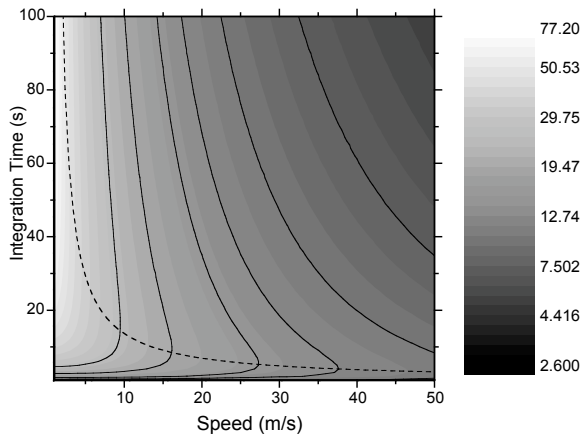


Fig. 1. SNR for a single detector; distance of closest approach = 20m, effective source activity = 0.01C. Shading represents SNR, according to color scale at right. Contour lines are at SNR values of 25, 20, 15, 12.5, 10, and 7.5. Dotted line defines locus of optimal integration times.

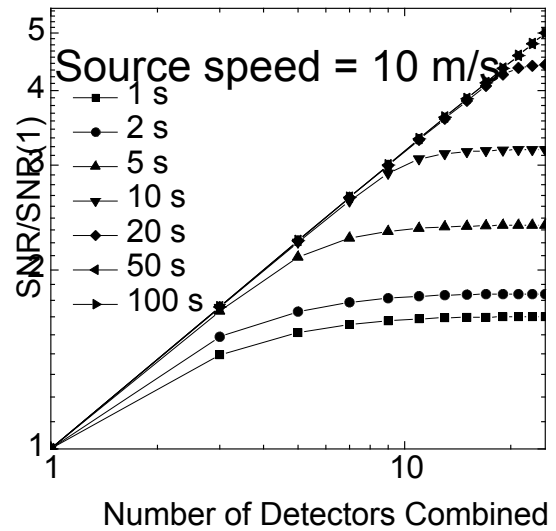
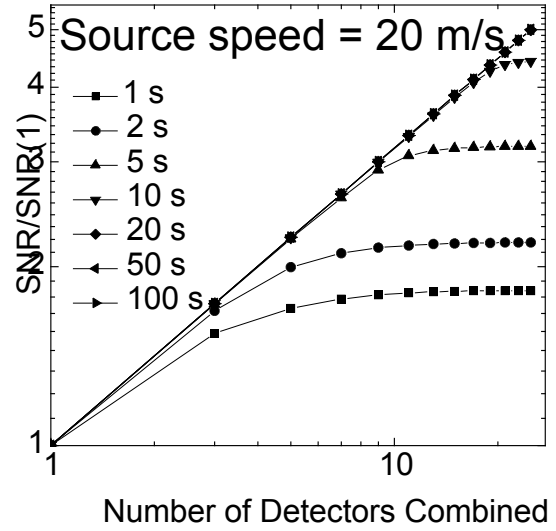


Fig. 2. SNR for multiple sensors ratioed to SNR for single sensor. Upper panel is for a source moving at 10 m/s; lower panel is for 20 m/s. Effective source activity is 0.01 C and distance of closest approach = 20 m. Legend gives integration time for each curve.

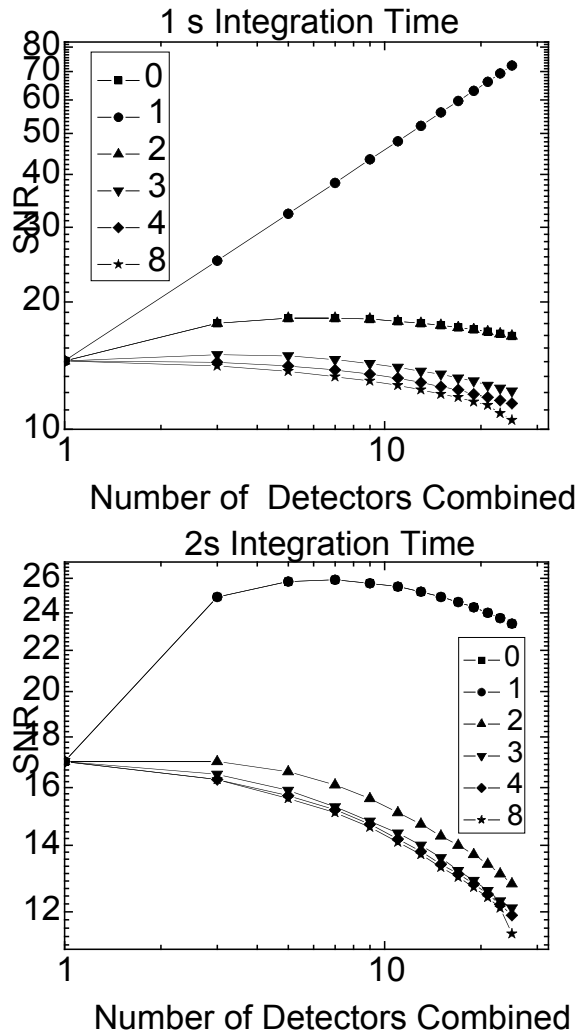


Fig. 3. SNR for detector outputs combined by coherent addition. Upper panel is for 1 s integration time, lower panel is for 2 s integration time. For both panels, source speed = 10 m/s, effective source activity = 0.001 C, distance of closest approach = 5 m. Legend gives Lag value for each curve.

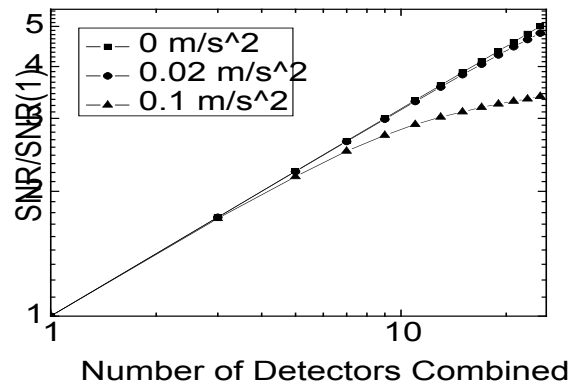


Fig. 4. SNR for detectors combined with coherent addition, including an acceleration term, ratioed to SNR for a single detector. Integration time = 1 s, effective source activity = 0.001 C, distance of closest approach = 5 m. The initial source speed was chosen such that the source was traveling at 10 m/s as it passed the 25th detector in the array, after an elapsed time of 100 s. Legend gives acceleration value for each curve.